

High-throughput Spheroid Formation and Migration with TeloCol-10 for Improved Stability

Paulo Godoy, PhD; Itedale Namro Redwan, PhD
Gothenburg, Sweden



Abstract

Type 1 collagen and Matrigel are gold standards for 3D cell culture and have recently been adapted for 3D bioprinting. However, there is still a knowledge gap regarding the scalability of natural matrices on bioprinted models for high-throughput spheroid formation and migration. In this application note, we demonstrate that type 1 collagen, in this case

[TeloCol®-10](#), supported breast cancer cell spheroid formation and migration with higher stability over longer incubation times compared to Matrigel under the same conditions. Although Matrigel is the gold standard and promotes the growth and migration of cells, droplets were easily detached during media exchange and signs of degradation were observed over time for the tested conditions.

Introduction

Among the natural matrices, collagen and Matrigel are considered gold standards for 3D cell culturing because of their ability to simulate *in vivo* cell-extracellular matrix (ECM) interactions. Matrigel offers many of the advantages of collagen and other natural hydrogels and has been used to study cell migration, angiogenesis and tumor development (Kleinman, 2005). It is derived from isolated ECM from the Engelbreth-Holm-Swarm mouse sarcoma and contains laminin, type 4 collagen, entactin, as well as several growth factors, cytokines and many other low abundant peptides/proteins, reaching 1851 proteins, identified by proteomics analysis (Hughes, 2010). Besides Matrigel's versatility, there are drawbacks that limit its use for drug discovery and disease modeling, including high batch-to-batch variation in composition (Hughes, 2010), tumor growth factors/peptides that may not be optimal for all organs or diseases (Mahoney, 2008), poor control over mechanical properties, and heterogeneous stiffness of samples (Reed, 2009).

Alternatively, collagen supports 3D cell culture without the cancer-derived growth factors and cytokines that Matrigel contains. Collagen is the

primary organic constituent of native tissues and among the 29 identified types, type 1 collagen is the most common (Shoulders, 2009). Due to their structural properties, biocompatibility, permeability and degradability, collagen-based hydrogels are ideal for replicating tissue development, regeneration and tumor biology (Sapudom, 2018).

TeloCol-10 contains 95% of type 1 collagen and 5% of type 3 (both of bovine origin). It preserves the telopeptide regions, resulting in increased stiffness, which offers more stability within the culture than atelocollagen (without the telopeptide). More stable hydrogels may benefit applications such as droplet-based spheroid formation and migration assays, which require longer incubation times as cellular behavior is monitored for several days before and after the addition of drugs. Furthermore, by changing TeloCol-10 concentration, its stiffness can be modulated to mimic different physiological conditions. Other studies have estimated the stiffness of breast cancer stroma to be around 400 to 1500 Pa, while normal breast tissue is around 150 Pa (Cox, 2011), similar values were obtained for 6 mg/mL (≈ 1200 Pa) and 4 mg/mL (≈ 230 Pa) of TeloCol-10 (**Figure 1**). Matrigel reached only 50 Pa when diluted to 6 mg/mL (Slater, 2021).

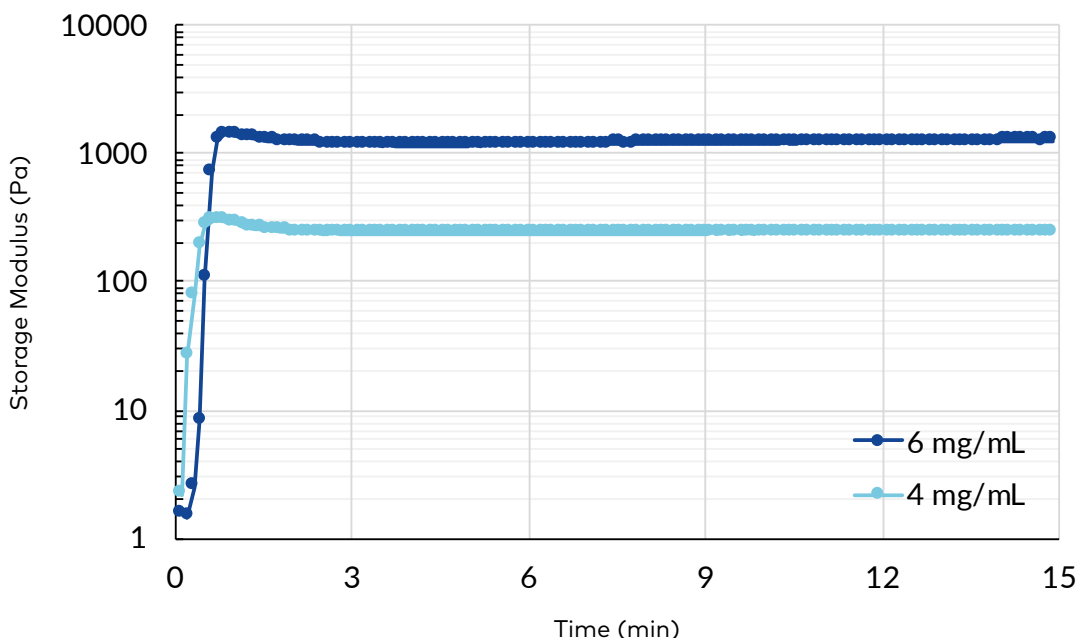


Figure 1. Storage modulus of TeloCol-10 diluted to 6 and 4 mg/mL.

APPLICATION NOTE

The 3D bioprinting revolution has made it possible to create reproducible 3D models in microplates (Blanco-Fernandez, 2021). However, there is still more to learn about the scalability and stability of natural matrices on bioprinted droplets for high-throughput spheroid formation and migration, and their use in drug discovery and tumor biology research.

We bioprinted droplets of cell-laden TeloCol-10 or Matrigel and monitored spheroid formation over 5 days using CYTENA's [CELLCYTE X™](#) live cell imaging system, which was also used to monitor the migration of cells from the inner core to the outer cell-free layer of bioprinted droplet-in-droplet structures (**Figure 2**).

In this application note, we compared the influence of type 1 collagen (TeloCol-10) and Matrigel on spheroid formation and migration of the breast cancer cell line MDA-MB-231, which is commonly used to model late-stage breast cancer because of its invasiveness.

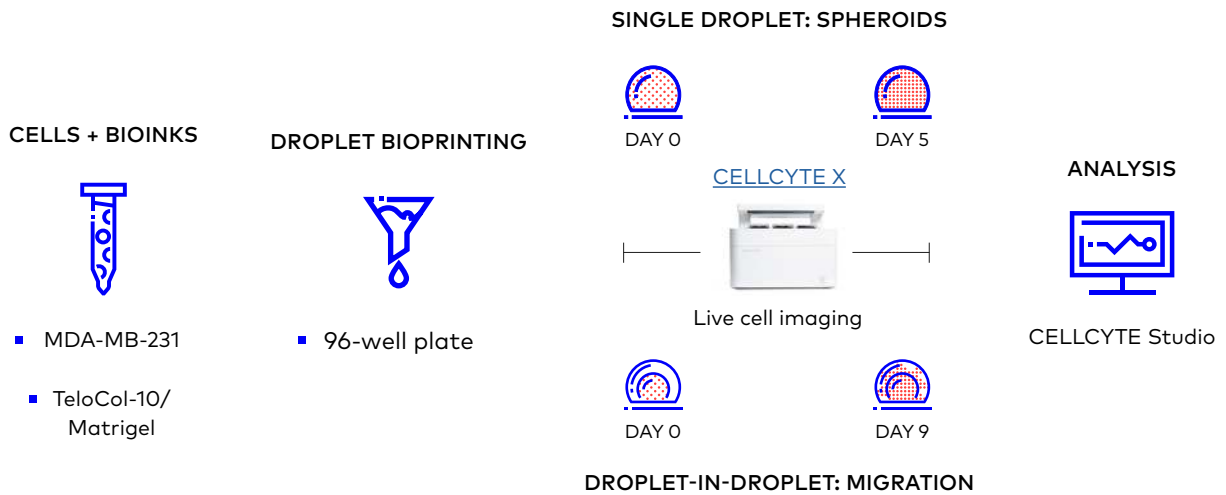


Figure 2. General workflow for TeloCol-10 or Matrigel 3D bioprinting of spheroid (droplet) and migration (droplet-in-droplet) models and analysis.

Materials and methods

Cell culture

MDA-MB-231 (ATCC, HTB-26) mCherry-tagged cells were cultured in complete Dulbecco's Modified Eagle Medium (DMEM) supplemented with 10% fetal bovine serum (FBS), 1% penicillin/streptomycin at 37°C with 5% CO₂ and 95% humidity. Cells were kept in monolayer culture prior to being embedded in TeloCol-10 (Advanced BioMatrix, 5226-20ML) or Matrigel (Corning, 354234). Cell suspensions with viability higher than 90% were used for bioprinting. The final cell concentration after mixing with TeloCol-10 or Matrigel was 4x10⁶ cells/mL.

Preprinting preparation

For each hydrogel, two different concentrations were used: 6 mg/mL for the spheroid formation assay and for the inner droplet in the migration assay, and 4 mg/mL for the outer droplet in the migration assay. All materials were kept on ice prior to the homogenization steps.

To obtain a final concentration of 4 and 6 mg/mL from TeloCol-10 (10 mg/mL), the solution was neutralized and diluted according to the manufacturer's protocol. The Matrigel (10.3 mg/mL) was only diluted using cell suspension. The hydrogel was mixed with the cell suspension using two 3 mL syringes, mixing back and forth 30 times.

Bioprinting protocol

The syringes containing TeloCol-10 or Matrigel with cells were capped with 22G conical nozzles and loaded into a custom biodispenser developed internally at CELLINK with a precooled printhead (2°C) and with a thermal insulator attached to it. A tissue culture-treated 96-well plate (Corning, 3599) was attached to the printbed. For the spheroid assay, 1 µL droplets were printed with cells embedded in 6 mg/mL of TeloCol-10 or Matrigel.

For the migration assay, 1 µL droplets were printed with cells embedded in 6 mg/mL of TeloCol-10 or Matrigel. After the droplets were printed, the plate was immediately placed in a 37°C humidified incubator for approximately 15 minutes for thermal crosslinking of TeloCol-10. The Matrigel plate was incubated for 25 minutes. After gelation of the first droplet, the outer droplet (5 µL) was printed with 4 mg/mL of TeloCol-10 or Matrigel and the thermal gelation inside the incubator was repeated. 300 µL medium was added to each well, and the constructs were incubated until downstream analysis. Half of the medium was replaced with fresh medium every 3 days.

Live cell imaging

The CELLCYTE X is a high-throughput live cell imaging system (with 3 fluorescence channels as well as bright-field) that can monitor cell viability in real time for long-term incubation. We implemented the spheroid analysis mode, which can be adapted to the collagen- or Matrigel-embedded cells. After adding medium to the printed droplets, the well plate was placed inside the CELLCYTE X and incubated for 30 minutes before imaging was started to minimize condensation. CELLCYTE Studio was set to capture every well in bright-field and red fluorescence at 4x magnification every 3 hours for 5 days.

Analysis

For the spheroid formation assay, the total red fluorescent data was compiled. The red fluorescence at specific time points was normalized to the initial red fluorescence at time 0. This normalization made it possible to compare the collagen and Matrigel results. While 59 droplets were analyzed for TeloCol-10, 52 droplets were analyzed for Matrigel. The migration assay was analyzed by comparing different migration patterns from TeloCol-10 or Matrigel-embedded cells in 12 constructs each.

Results and discussion

Bioprinting of tumor spheroids

One of the simplest bioprinted models consists of cells embedded in hydrogel droplets dispensed in well plates, where cells aggregate spontaneously into spheroids. Here, we used the MDA-MB-231 mCherry-tagged breast cancer cells embedded in TeloCol-10 or Matrigel at 6 mg/mL with 4×10^6 cells/mL, bioprinted as 1 μ L droplet in 96-well plates. From day 1 to 5, droplets were imaged with the CELLCYTE X, which captured bright-field and red fluorescent images at 4x magnification. The breast cancer cells grew consistently in TeloCol-10, forming aggregates and spheroids after day 3, and maintained consistent growth until day 5 (**Figure 3A**). In Matrigel (**Figure 3B**), the cells aggregated into spheroids by day 2.

Starting on day 3, the Matrigel droplet started to degrade at the edges, pushing the cell clusters to the center while leaving the cells growing on the well plastic. On day 4 and 5, all small spheroid clusters had merged into a large central cluster, while the cells attached to the flask had overgrown and occupied most of the well area. Interestingly, the red fluorescence captured every 3 hours through the entire process showed that the cells in Matrigel and TeloCol-10 grew at the same rate (**Figure 4**).

For drug testing protocols, cells are typically treated 3 to 7 days after printing, when 3D structures are formed. Here, we demonstrated that the TeloCol-10 had more stability for this specific setup. To further evaluate the influence of Matrigel or TeloCol-10 in more complex cellular models, we adapted a migration protocol using two different hydrogel stiffnesses.

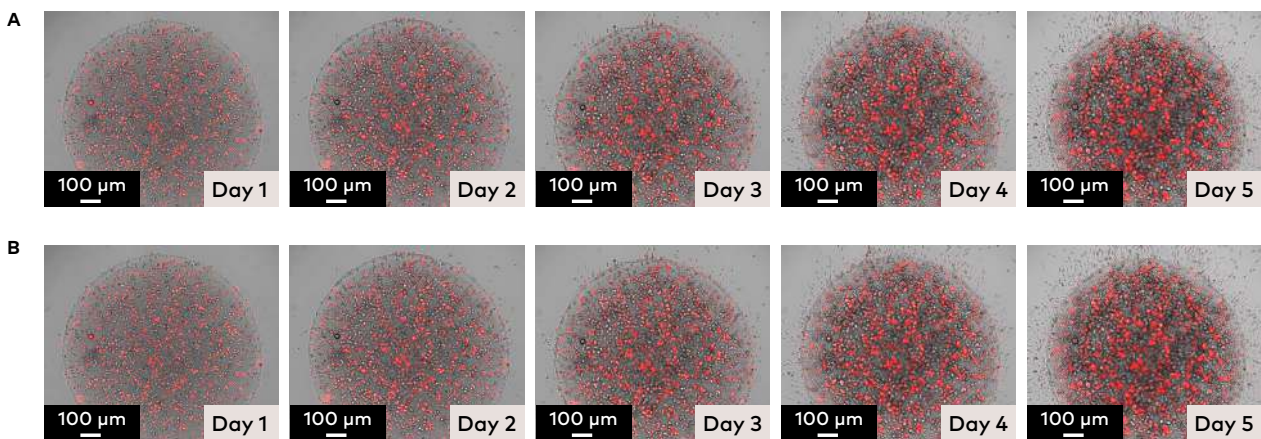


Figure 3. Representative pictures of live MDA-MB-231 mCherry (red) embedded in **A)** TeloCol-10 (6 mg/mL), or **B)** Matrigel (6 mg/mL) bioprinted in 1 μ L droplets. Cells were monitored for 5 days using the CELLCYTE X system (4x, bright-field and red fluorescence). Spheroids were formed on both hydrogels while droplet degradation was only evident in Matrigel after day 3.

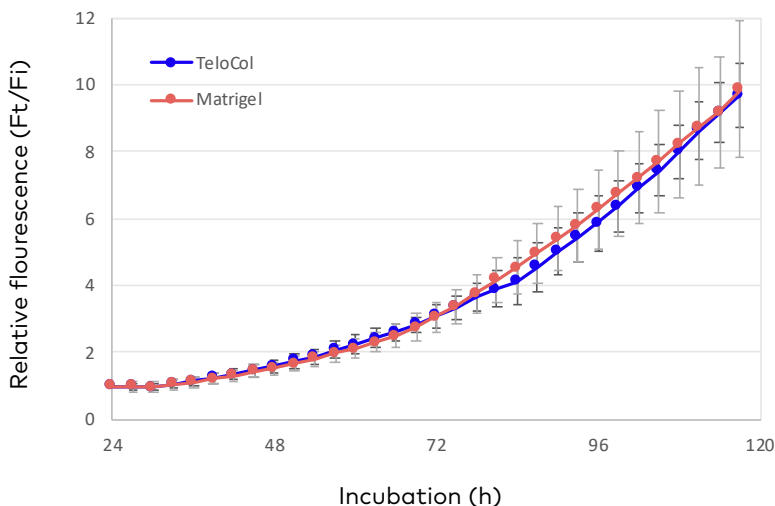


Figure 4. Relative red fluorescence analysis of TeloCol-10 (6 mg/mL) and Matrigel (6 mg/mL) droplets containing MDA-MB-231 mCherry cells. Cells were monitored from days 1 to 5 by the CELLCYTE X system, where images were acquired at 4x magnification using bright-field and red fluorescence. Relative fluorescence (F_t/F_i). F_t : Total red fluorescence at specific time; F_i : total red fluorescence at time 0.

Cancer cell invasion in different matrices

We adapted a previously tested droplet-in-droplet method to study the influence of different hydrogel concentrations. The assay entails a central core droplet embedded with cells, covered by a cell-free outer droplet (Takata, 2009; Zaman, 2006). In this assay, we bioprinted 1 μL droplets of TeloCol-10 (6 mg/mL) or Matrigel (6 mg/mL) containing 4×10^6 cells/mL into 96-well plates to create the central core embedded with cells. After polymerization of the first droplet, the second cell-free droplet of TeloCol-10 (4 mg/mL) or Matrigel (4 mg/mL) was printed over the core droplet. The migration model was tracked with the CELLCYTE X every 3 hours for 9 days (Figure 5).

The initial migration of cells out of the inner droplet to the cell-free outer droplet for TeloCol-10 and Matrigel could be observed after 3 days and was followed by a massive migration on subsequent days. Furthermore, degradation of the inner layer as the cells migrated out enabled the central formation of spheroid clusters, like the degradation observed in the spheroid model. On day 7, the outer layer of Matrigel also started to degrade and contract, moving to the same central area and leaving a track of cells attached to the bottom of the well. Overall, we were able to track the migrating cells in the TeloCol-10 model for up to 9 days, while cells in the Matrigel model had reached the border of the outer layer on day 7.

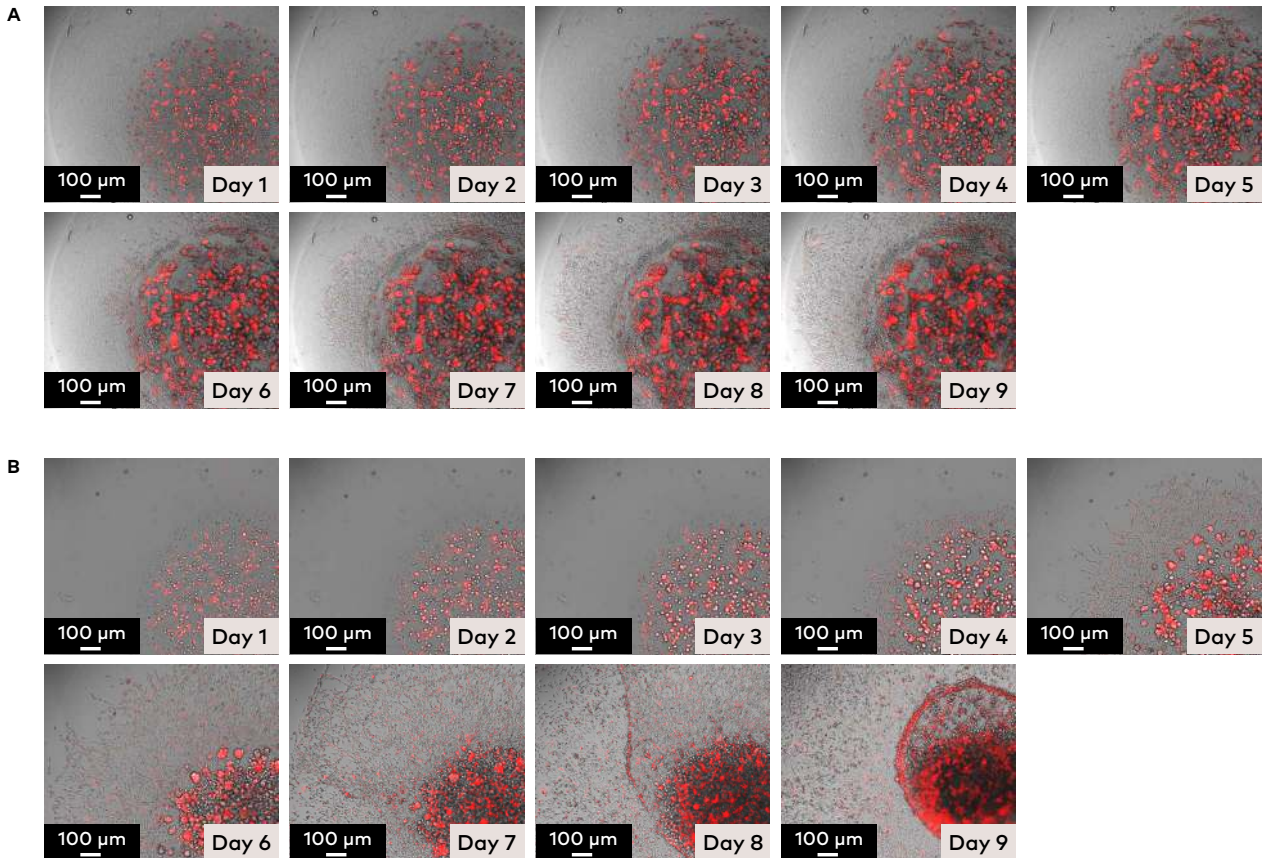


Figure 5. Droplet-in-droplet model for cancer cell migration. The inner core contains live MDA-MB-231 mCherry (4×10^6 cells/mL in red) embedded in **A**) TeloCol-10 (6 mg/mL) or **B**) Matrigel (6 mg/mL) in 1 μL droplets followed by 5 μL cell-free TeloCol-10 or Matrigel (4 mg/mL) covering the inner droplet. Cells were monitored for 9 days by the CELLCYTE X system (4x bright-field and red fluorescence). Droplet degradation was evident only in Matrigel.

Degradation of Matrigel

The Matrigel degradation observed in both the spheroid formation and migration assay has been linked to proteolytical digestion by the growing cells (Lee, 2007; Albini and Benelli, 2007). The small droplet volume of 1 μ L, the hydrogel concentration of 4 to 6 mg/mL and high cellular concentration could also have contributed to this degradation. When used in thin layers, Matrigel has been shown to form abnormal structures and exhibit a tendency for cells to grow as monolayers (Belfiore, 2021). In addition, Matrigel also has variations in protein and growth factor composition that have been shown to affect mechanical properties of the gel, cell growth, migration and experiment reproducibility (Caliari, 2016; Aisenbrey, 2020; Morales, 2021). In previous experiments, Matrigel droplets have detached from the bottom of the well during the changing of medium or when drugs are added (data not shown), while TeloCol-10 droplets steadily adhered to the center of the well.

One of the main contributing factors to the stability of TeloCol-10 is the moderate stiffness (1.2 kPa) achieved when diluted from 10 mg/mL to 6 mg/mL, compared to the 50 Pa reached by polymerized Matrigel at the same concentration (Slater, 2021). TeloCol-10 preserves the telopeptide regions of collagen, which offer an additional crosslinking point between fibers and result in increased stiffness (Woodley, 1991). Furthermore, TeloCol-10 has more than 99% purity while Matrigel is known to have multiple active growth factors, which may influence cellular activity, requiring users to use caution when interpreting the latter (Vukicevic, 1992).

Conclusion

- TeloCol-10 supports both breast cancer spheroid formation and migration with similar growth rates as Matrigel at the same concentrations.
- Matrigel at 6 mg/mL presented degradation after 4 days in the tumor spheroid assay, and after 6 and 7 days for inner (6 mg/mL) and outer droplets (4 mg/mL) in the cancer cell migration assay. The TeloCol-10 showed no sign of degradation in either assay.
- High-stiffness collagen in TeloCol-10 keeps the droplet structure stable over longer incubation times and contains fewer growth factors than Matrigel, which makes TeloCol-10 the better choice for high-throughput bioprinting.

References

1. Aisenbrey EA, Murphy WL. Synthetic alternatives to Matrigel. *Nature Reviews Materials*. 2020; 5(7): 539–551. [DOI:10.1038/s41578-020-0199-8](https://doi.org/10.1038/s41578-020-0199-8).
2. Albini A, Benelli R. The chemoinvasion assay: A method to assess tumor and endothelial cell invasion and its modulation. *Nature Protocols*. 2007; 2(3): 504–511. [DOI:10.1038/nprot.2006.466](https://doi.org/10.1038/nprot.2006.466).
3. Blanco-Fernandez B, Gaspar VM, Engel E, Mano JF. Proteinaceous hydrogels for bioengineering advanced 3D tumor models. *Advanced Science*. 2021; 8(4): 2003129. [DOI:10.1002/advs.202003129](https://doi.org/10.1002/advs.202003129).
4. Caliari SR, Burdick JA. A practical guide to hydrogels for cell culture. *Nature Methods*. 2016; 13(5): 405–414. [DOI:10.1038/nmeth.3839](https://doi.org/10.1038/nmeth.3839).
5. Cox TR, Ertler JT. Remodeling and homeostasis of the extracellular matrix: Implications for fibrotic diseases and cancer. *Disease Models & Mechanisms*. 2011; 4(2): 165–178. [DOI:10.1242/dmm.004077](https://doi.org/10.1242/dmm.004077).
6. Hongisto V, Jernström S, Fey V, et al. High-throughput 3D screening reveals differences in drug sensitivities between culture models of JIMT1 breast cancer cells. *PLoS One*. 2013; 8(10): e77232. [DOI:10.1371/journal.pone.0077232](https://doi.org/10.1371/journal.pone.0077232).
7. Hughes CS, Postovit LM, Lajoie GA. Matrigel: A complex protein mixture required for optimal growth of cell culture. *Proteomics*. 2010; 10(9): 1886–1890. [DOI:10.1002/pmic.200900758](https://doi.org/10.1002/pmic.200900758).
8. Kleinman HK, Martin GR. Matrigel: Basement membrane matrix with biological activity. *Seminars in Cancer Biology*. 2005; 15(5): 378–386. [DOI:10.1016/j.semcancer.2005.05.004](https://doi.org/10.1016/j.semcancer.2005.05.004).
9. Kozłowski MT, Crook CJ, Ku HT. Towards organoid culture without Matrigel. *Communications Biology*. 2021; 4(1): 1387. [DOI:10.1038/s42003-021-02910-8](https://doi.org/10.1038/s42003-021-02910-8).
10. Lee GY, Kenny PA, Lee EH, Bissell MJ. Three-dimensional culture models of normal and malignant breast epithelial cells. *Nature Methods*. 2007; 4(4): 359–365. [DOI:10.1038/nmeth1015](https://doi.org/10.1038/nmeth1015).
11. Li Y, Kumacheva E. Hydrogel microenvironments for cancer spheroid growth and drug screening. *Science Advances*. 2018; 4(4). [DOI:10.1126/sciadv.aas8998](https://doi.org/10.1126/sciadv.aas8998).
12. Lobo DA, Ginestra P, Ceretti E, et al. Cancer cell direct bioprinting: A focused review. *Micromachines*. 2021; 12(7): 764. [DOI:10.3390/mi12070764](https://doi.org/10.3390/mi12070764).
13. Mahoney ZX, Stappenbeck TS, Miner JH. Laminin alpha 5 influences the architecture of the mouse small intestine mucosa. *Journal of Cell Science*. 2008; 121(Pt 15): 2493–2502. [DOI:10.1242/jcs.025528](https://doi.org/10.1242/jcs.025528).
14. Morales X, Cortés-Domínguez I, Ortiz-de-Solorzano C. Modeling the mechanobiology of cancer cell migration using 3D biomimetic hydrogels. *Gels*. 2021; 7(1): 17. [DOI:10.3390/gels7010017](https://doi.org/10.3390/gels7010017).
15. Ray A, Morford RK, Ghaderi N, et al. Dynamics of 3D carcinoma cell invasion into aligned collagen. *Integrative Biology*. 2018; 10(2): 100–112. [DOI:10.1039/c7ib00152e](https://doi.org/10.1039/c7ib00152e).
16. Reed J, Walczak WJ, Petzold ON, Gimzewski JK. In situ mechanical interferometry of matrigel films. *Langmuir: The ACS Journal of Surfaces and Colloids*. 2009; 25(1): 36–39. [DOI:10.1021/la8033098](https://doi.org/10.1021/la8033098).
17. Sapudom J, Pompe T. Biomimetic tumor microenvironments based on collagen matrices. *Biomaterials Science*. 2018; 6(8): 2009–2024. [DOI:10.1039/c8bm00303c](https://doi.org/10.1039/c8bm00303c).
18. Shoulders MD, Raines RT. Collagen structure and stability. *Annual Review of Biochemistry*. 2009; 78(1): 929–958. [DOI:10.1146/annurev.biochem.77.032207.120833](https://doi.org/10.1146/annurev.biochem.77.032207.120833).
19. Slater K, Partridge J, Nandivada H. Tuning the elastic moduli of Corning Matrigel and collagen I 3D matrices by varying the protein concentration. Corning Incorporated Application Note CLS-AC-AN-449 REV1. <https://www.corning.com/catalog/cls/documents/application-notes/CLS-AC-AN-449.pdf> Accessed February 9, 2022.
20. Takata M, Maniwa Y, Doi T, et al. Double-layered collagen gel hemisphere for cell invasion assay: Successful visualization and quantification of cell invasion activity. *Cell Communication and Adhesion*. 2007; 14(4): 157–167. [DOI:10.1080/15419060701557859](https://doi.org/10.1080/15419060701557859).

21. Thakuri PS, Liu C, Luker GD, Tavana H. Biomaterials-based approaches to tumor spheroid and organoid modeling. *Advanced Healthcare Materials*. 2017; 7(6): 1700980. [DOI:10.1002/adhm.201700980](https://doi.org/10.1002/adhm.201700980).
22. Tuomainen K, Al-Samadi A, Potdar S, et al. Human tumor-derived matrix improves the predictability of head and neck cancer drug testing. *Cancers*. 2020; 12(1): 92. [DOI:10.3390/cancers12010092](https://doi.org/10.3390/cancers12010092).
23. Vukicevic S, Kleinman HK, Luyten FP, et al. Identification of multiple active growth factors in basement membrane Matrigel suggests caution in interpretation of cellular activity related to extracellular matrix components. *Experimental Cell Research*. 1992; 202(1): 1–8. [DOI:10.1016/0014-4827\(92\)90397-q](https://doi.org/10.1016/0014-4827(92)90397-q).
24. Woodley D, Yamauchi M, Wynn K, et al. Collagen telopeptides (cross-linking sites) play a role in collagen gel lattice contraction. *Journal of Investigative Dermatology*. 1991; 97(3): 580–585. [DOI:10.1111/1523-1747.ep12481920](https://doi.org/10.1111/1523-1747.ep12481920).
25. Zaman MH, Trapani LM, Sieminski AL, et al. Migration of tumor cells in 3D matrices is governed by matrix stiffness along with cell-matrix adhesion and proteolysis. *Proceedings of the National Academy of Science of the United States of America*. 2006; 103(29): 10889–10894. [DOI:10.1073/pnas.0604460103](https://doi.org/10.1073/pnas.0604460103).
26. Zhu M, Wang Y, Ferracci G, et al. Gelatin methacryloyl and its hydrogels with an exceptional degree of controllability and batch-to-batch consistency. *Scientific Reports*. 2019; 9(1): 6863. [DOI:10.1038/s41598-019-42186-x](https://doi.org/10.1038/s41598-019-42186-x).



Read other
application notes

©2022 BICO AB. All rights reserved. Duplication and/or reproduction of all or any portion of this document without the express written consent of BICO is strictly forbidden. Nothing contained herein shall constitute any warranty, express or implied, as to the performance of any products described herein. Any and all warranties applicable to any products are set forth in the applicable terms and conditions of sale accompanying the purchase of such product. BICO provides no warranty and hereby disclaims any and all warranties as to the use of any third-party products or protocols described herein. The use of products described herein is subject to certain restrictions as set forth in the applicable terms and conditions of sale accompanying the purchase of such product. BICO may refer to the products or services offered by other companies by their brand name or company name solely for clarity and does not claim any rights to those third-party marks or names. BICO products may be covered by one or more patents. The use of products described herein is subject to BICO's terms and conditions of sale and such other terms that have been agreed to in writing between BICO and user. All products and services described herein are intended FOR RESEARCH USE ONLY and NOT FOR USE IN DIAGNOSTIC PROCEDURES.

The use of BICO products in practicing the methods set forth herein has not been validated by BICO, and such nonvalidated use is NOT COVERED BY BICO'S STANDARD WARRANTY, AND BICO HEREBY DISCLAIMS ANY AND ALL WARRANTIES FOR SUCH USE. Nothing in this document should be construed as altering, waiving or amending in any manner BICO's terms and conditions of sale for the instruments, consumables or software mentioned, including without limitation such terms and conditions relating to certain use restrictions, limited license, warranty and limitation of liability, and nothing in this document shall be deemed to be Documentation, as that term is set forth in such terms and conditions of sale. Nothing in this document shall be construed as any representation by BICO that it currently or will at any time in the future offer or in any way support any application set forth herein.